

A new biocompatible delivery scaffold containing heparin and bone morphogenetic protein 2

SUPHANNEE THANYAPHOO¹
JASADEE KAEWSRICHAN^{2*}

¹Department of Pharmaceutical
Chemistry
Faculty of Pharmaceutical Sciences
Prince of Songkla University
Hat-yai, Songkhla, Thailand

²Department of Pharmaceutical
Chemistry
Faculty of Pharmaceutical Sciences
and Nanotec-PSU Center of Excellence
on Drug Delivery System
Prince of Songkla University
Hat-yai, Songkhla, Thailand

Silicon-substituted calcium phosphate (Si-CaP) was developed in our laboratory as a biomaterial for delivery in bone tissue engineering. It was fabricated as a 3D-construct of scaffolds using chitosan-trisodium polyphosphate (TPP) cross-linked networks. In this study, heparin was covalently bonded to the residual $-NH_2$ groups of chitosan on the scaffold applying carbodiimide chemistry. Bonded heparin was not leached away from scaffold surfaces upon vigorous washing or extended storage. Recombinant human bone morphogenetic protein 2 (rhBMP-2) was bound to conjugated scaffolds by ionic interactions between the negatively charged SO_4^{2-} clusters of heparin and positively charged amino acids of rhBMP-2. The resulting scaffolds were inspected for bone regenerative capacity by subcutaneous implanting in rats. Histological observation and mineralization assay were performed after 4 weeks of implantation. Results from both *in vitro* and *in vivo* experiments suggest the potential of the developed scaffolds for bone tissue engineering applications in the future.

Keywords: heparin, carbodiimide, rhBMP-2, delivery scaffold, bone tissue engineering

Accepted March 1, 2016
Published online March 24, 2016

A critical size defect in bone is defined as a defect that will not heal without intervention (1). Bone tissue engineering is a strategy for completing bone regeneration in case of such defects. It relies on the complex interplay between cells, biomaterials and biomodulators, in intimate synergy with the hosts' biological capabilities. Unlike enamel and dentin, bone is a very dynamic tissue because modeling and remodeling processes occur simultaneously. Modeling is concerned with changes in bone shape, while remodeling implies bone turnover without shape modification. These operations take place through an organized sequence of events at the same anatomical location and are regulated by osteoblast and osteoclast activities, respectively (2). A variety of biomaterials have been developed to elicit an adequate response from the biological milieu. The response, if insufficient, may contribute to poor reactivity within direct contact of the damaged tissues, resulting in non-union.

* Correspondence; e-mail: jasadee.k@psu.ac.th

Bone morphogenetic proteins (BMPs) were introduced into clinical practice in the late 1990s, but only some have the potential to induce formation of new bone (3). BMP-2, trade name INFUSE® (Medtronic, MN, USA), received approval of US-FDA in 2002 for restricted use in the treatment of open tibial fractures and spinal fusion. However, it is often used off label to stimulate bone defect healing, not only in the upper and lower extremities but in craniofacial surgery as well. Regrettably, FDA issued a warning about the protein product six years later concerning the troublesome formation of bone in unwanted locations, and the potential to fuel the growth of cancer cells or spark adverse immune system reactions (4–6).

Use of scaffolds as a delivery system in bone tissue engineering is advantageous, because they can release an active agent in the exact area requested over a sustained period of time and can prevent leaching away of the entrapped compound from the desired site into the surrounding tissues (7, 8). Moreover, biomaterials as scaffold compositions can be optimized to support basic cellular functions by establishing an adequate framework for specific cell adhesion, proliferation and differentiation, leading to improved bone growth. Partial substitution of silicon (Si) atoms in crystal lattices of calcium phosphate (CaP) served as a rationale for enhancing bone regenerative capacity of biomaterials like CaP compounds (9). According to this scheme, new Si-substituted CaP, namely 0.4Si-synHA, has been synthesized in our laboratory and successfully used as a delivery scaffold for vancomycin (10). In fact, these scaffolds can be proposed for critical bone injury if bone related growth factors are coexistent and their sustained release characteristics are achievable. A new delivery system bearing recombinant human BMP-2 (rhBMP-2) was thus developed in this study. Carbodiimide chemistry was applied for bonding heparin to the scaffolds by ionic interactions to create rhBMP-2 binding sites (11). Therefore, it was essential (i) to determine the feasibility and efficiency of the coupling reaction when it was first applied to pair heparin and chitosan bearing scaffolds, (ii) to assess the binding affinity and release property of rhBMP-2 to and from the scaffolds *in vitro*, and (iii) to verify the ability of the scaffolds in bone regeneration *in vivo*. All approaches introduced are aimed at acquiring biocompatible rhBMP-2 delivery scaffolds for effective bone regeneration capacity of critical bone defects.

EXPERIMENTAL

Materials, chemicals, assay kits and accessories

The Si-substituted CaP compound 0.4Si-synHA was synthesized in our laboratory according to the procedures described previously (10). It was fabricated as a 3D-construct of scaffolds and was used throughout the study. Chitosan from crab shells (M_r 140,000–200,000, deacetylation degree ~80 %) was a commercial product of Sigma (USA). Sodium tripolyphosphate (TPP) was acquired from Sigma-Aldrich (Germany). Heparin (M_r ~5000) and chemicals for the heparin conjugation process, *N*-(3-dimethylaminopropyl)-*N'*-ethylcarbodiimide hydrochloride (EDC), *N*-hydroxysuccinimide (NHS), and 2-morpholino-ethane sulfonic acid (MES), were purchased from Sigma. rhBMP-2 was supplied in a homodimeric form (M_r 26 000) by BioVision (USA). Bovine serum albumin (BSA) was obtained from Sigma-Aldrich. Staining dyes, including hematoxylin/eosin (H&E) and alizarin red S, were also purchased from Sigma-Aldrich. Other chemicals were of analytical grade and were acquired from Merck (Germany). The Quantikine® BMP2 ELISA kit was a

commercial product of R&D Systems (USA), and the mineralization assay kit was supplied by Interchim (USA). A 250- μL measuring micro-syringe (Hamilton®) was obtained from Hamilton Company (USA).

Preparation of scaffolds

Five grams of 0.4Si-synHA powder were triturated with 1 mL of chitosan solution (1.5 % *m/V* in 3 % *V/V* acetic acid) until a smooth paste was obtained. The paste was molded into an open-end plastic tube of 5 mm diameter \times 3 mm length and left at room temperature to dry. Dried paste in the mold was immersed in sodium tripolyphosphate (TPP) solution (1 % *m/V* in 3 % *V/V* acetic acid) at room temperature for 24 h to allow crosslinking of chitosan and TPP (12). After that, the plastic mold was carefully trimmed out and the scaffold was thoroughly washed with distilled water. Any trapped water in the scaffold was removed by freeze-drying (ROCTEC, Hong Kong). A scaffold of an average mass of 0.4 g was obtained. It was stored at 4 °C until use unless otherwise stated.

Conjugation of heparin onto the scaffold

MES buffer was prepared by dissolving 0.433 g EDC and 0.157 g NHS in 188.3 mL water and adjusted to pH 5.4. A certain amount of heparin was dissolved in this buffer to a concentration of 1, 2, or 4 mmol L^{-1} . Before use, the MES buffer and heparin solutions were sterilized by filtering through a 0.2- μm membrane filter. Twelve pieces of prepared scaffolds, total mass 5 g, were sterilized by soaking in 70 % ethanol for 1 h, left to air-dry, and subsequently incubated in the MES solution for 30 min for activation. After being removed and placed on a sterile paper to discard any residual buffer, a group of four pieces of these activated scaffolds were immersed in a tube containing 200 μL of heparin solution. The existing air bubble was evacuated using a vacuum pump at 200 Pa for 30 s, and incubation was carried out at 37 °C for a further 4 h. Excess supernatant was then fully drawn out using a 250- μL measuring micro-syringe and stored at 4 °C until use for determination of unreacted heparin. The scaffold was washed with a series of sterile sodium chloride solutions (*i.e.*, 2 mol L^{-1} , 6 times for 4 h, and 4 mol L^{-1} , 4 times for 6 h) and then with sterile water (3 times for 8 h). After freeze-drying, the heparin-conjugated scaffolds were kept in a sterile container at 4 °C until use. Each experiment was performed in triplicate.

Characterization of the heparin-conjugated scaffold

Contents of conjugated heparin. – Heparin bound on the conjugated scaffold was qualitatively investigated using the toluidine blue method (13). Briefly, 0.4 mg mL^{-1} toluidine blue solution in 0.1 mol L^{-1} hydrochloric acid containing 0.2 % *m/V* sodium chloride was prepared. The test scaffold was immersed in the dye solution for 4 h at room temperature under gentle agitation using a vortex. The scaffold was then removed, placed on filter paper to give up excess dye, washed with distilled water (2 times for 5 min), and air-dried. The stained scaffold was photographed using a Canon PowerShot G3X camera.

The method of Smith *et al.* (14) was applied for precise determination of the heparin content bound on the scaffold. 50 μL of the collected supernatant was added to a test tube containing 950 μL of toluidine blue solution (prepared as described above) and incubated at room temperature for 30 min under gentle shaking. Four milliliters of *n*-hexane was

then added and mixed for 30 s using a vortex, followed by centrifugation at 2,000 rpm for 2 min. The aqueous layer was aspirated, diluted 1:10 with ethanol, and OD_{630} was measured within 30 min. The heparin calibration curve was prepared as follows. Varying volumes of 2 mmol L⁻¹ heparin solution were separately added to each of 5 tubes containing 950 μ L of toluidine blue solution and the volume of 1 mL was made up by addition of 0.2 % *m/V* sodium chloride. The following steps were performed in a similar ways as described previously. Heparin content per scaffold was calculated taking into account the concentration of heparin solution before and after incubation with the scaffolds.

Stability of conjugated bonds. – Pig whole blood was obtained from the slaughter-house authorized by the Faculty of Natural Resources, Prince of Songkla University. A fraction, called platelet-rich plasma (PRP), was prepared by mixing 1 volume of blood and 9 volumes of 3.8 % *m/V* tri-sodium citrate solution in a plastic tube. The PRP jelly was separated by centrifugation at 1300 rpm for 10 min at 4 °C. The heparin-conjugated scaffold was shaken vigorously in PBS and PBS was collected for the assay of heparin bonding stability. The collected PBS was incubated with the PRP for 30 min at 37 °C under static conditions. Clotting appearance was visually observed and recorded as ++, + or – for truly clotted, slightly clotted or unclotted status of the PRP.

Loading of rhBMP-2

rhBMP-2 protein was reconstituted to a concentration of 1 mg mL⁻¹ (38.5 mmol L⁻¹) in water containing 50 mg mL⁻¹ BSA according to the manufacturer's recommendation. This solution was further diluted to a concentration of 0.4 or 0.8 μ mol L⁻¹ in PBS, filter sterilized and stored in aliquot amounts at –20 °C until use. Four pieces of conjugated scaffolds in each defined group were continually used for rhBMP-2 loading. One day before implantation, the scaffolds were immersed in a tube containing 200 μ L of rhBMP-2 solution and incubated at 4 °C for an additional 24 h. Excess protein solution was completely drawn out using a micro-titrating syringe and stored at 4 °C until use for determination of the amounts of unbound rhBMP-2. The obtained scaffolds were subsequently transplanted into rats. Each experiment was done in triplicate.

Characterization of rhBMP-2 loaded scaffolds

Determination of bound rhBMP-2. – The amount of rhBMP-2 bound to each scaffold was indirectly assayed in the excess protein solution collected using the Quantikine® BMP-2 ELISA kit. In brief, 100 μ L of the test solution was added to a well of BMP-2 antibody precoated microplate and incubated for 2 h at room temperature. Added solution was then removed and the well was washed 4 times with washing buffer, followed by the addition of horseradish peroxidase conjugated BMP-2 antibody. After 2 h of incubation at room temperature, the antibody solution was aspirated and the well was completely washed with washing buffer. Then, tetramethylbenzidine substrate was added and incubated for 30 min in the dark before stop solution was added to terminate the reaction. The OD_{450} was measured within 30 min. The BMP-2 standard curve was prepared according to the manufacturer's recommendation. The rhBMP-2 content per scaffold was calculated taking into account the concentration of rhBMP-2 solution before and after incubation with scaffolds.

Release of rhBMP-2 in vitro. – The release of rhBMP-2 from finished scaffolds was performed in PBS at 4 °C under static conditions. Briefly, four pieces of these scaffolds in each defined group, total mass ~2 g, were immersed in each of six tubes containing 500 µL of PBS. The tubes were separately incubated at 4 °C without agitation for a desired time period of 3, 7, 10, 14, 28 or 45 days. At each specified time period, 100 µL of the supernatant were aspirated and stored at 4 °C until use. The amount of rhBMP-2 released from the scaffolds was determined using the ELISA kit. Results were calculated by comparison with the standard curve and were reported as % release.

Animals, surgical procedure and implantation

The experiment involving animals was approved by the PSU animal care and use committee of the Prince of Songkla University. Four male 8-week-old Wistar rats (mass 220–250 g) were anesthetized by intramuscular injection of the mixture containing a 1:1 volume ratio of xylazine (25 mg mL⁻¹) and zoletil (12.5 mg mL⁻¹) at a dose of 100 µL per 100 g body mass. The animal lumbar area was disinfected and shaved. Seven pockets, each 6 mm wide, were created and a test implant was inserted into each. Seven different groups of implants were formed according to the concentrations of heparin and rhBMP-2 was used in the conjugation reaction and the loading process. The groups included Gr.1, 0/0; Gr. 2, 1/0; Gr. 3, 1/0.4; Gr. 4, 1/0.8; Gr. 5, 2/0; Gr. 6, 2/0.4; and Gr. 7, 2/0.8, where the first number was heparin concentration in mmol L⁻¹ and the last number was rhBMP-2 concentration in µmol L⁻¹. The wounds were closed using 4–0 silk sutures and a topical antibiotic was applied to operated rats for 1 week.

Histological analysis

After 4 weeks of implantation, the animals were sacrificed and the implants were excised. The excised implant was fixed in 10 % V/V formaldehyde in PBS for 24 h and decalcified in 1 mol L⁻¹ HCl saturated with EDTA for 2 days. The decalcified sample was paraffin embedded, sectioned to 5-µm thick layers, and separately stained with hematoxylin/ eosin (H&E) and alizarin red S. Three different levels of each section were collectively analyzed using Cell P Software on a light microscope (Olympus).

Mineralization assay

All forms of calcium deposited on a sectioned implant were quantitatively determined using the Interchim mineralization assay kit after alizarin red S staining. The stained sample was placed in a well of a 24-well plate and incubated with 500 µL of stain solubilizing solution for 10 min. Then, 150 µL of the supernatant was transferred to a well of a 96-well plate, repeated three times and measured for OD₄₀₅. The dye standard curve was prepared using alizarin red S in a concentration range of 5–500 µg mL⁻¹. Results were calculated by comparison with the dye standard curve and reported in µg mL⁻¹ of alizarin red S stained per section.

Statistical analysis

Data were presented as means ± standard deviation (SD) with $n = 3$ for the *in vitro* experiments, and $n = 6$ for the *in vivo* study. Statistical analyses were carried out by ANO-

VA (analysis of variance) using the Statistics Package for Social Science (SPSS) software. Differences were considered statistically significant at $p < 0.05$. All histological analyses were performed by two independent observers.

RESULTS AND DISCUSSION

Conjugation efficiency and stability of heparin conjugates

Chitosan (pK_a 6.3) is polycationic when dissolved in acids and presents $-\text{NH}_3^+$ sites, while TPP dissociated in acids gives phosphoric anions. Hence, in acidic pH, these oppositely charged moieties can be associated by ionic interactions (12). For this reason, a 3D-construct of scaffolds was created in the present study. With the chitosan to TPP concentration ratio as specified, some $-\text{NH}_3^+$ groups of chitosan remained unreacted and became $-\text{NH}_2$ when the acid was washed off with distilled water (15). In the MES buffer containing EDC and NHS reagents, residual $-\text{NH}_2$ groups of chitosan and $-\text{COOH}$ groups of added heparin were activated and concurrently conjugated, forming surfaced heparin scaffolds according to the carbodiimide chemistry principle (16). The resulting products were later named conjugated scaffolds. In fact, this chemical reaction was employed to bridge heparin with gelatin (17) and heparin with collagen (18). Interestingly, it was first applied in this study for bonding heparin to chitosan present on the scaffolds.

The toluidine blue method developed by Dick *et al.* was chosen for qualitative determination of surfaced heparin, because it not only gives specific and homogeneous stain but is also less sensitive to artifacts (13). Results are shown in Fig. 1. The control was free of heparin conjugation and was not stained with the dye (Fig. 1a). Indeed, the dye specifically stained the heparin containing samples with homogeneous dye color (Fig. 1b–d). Besides the suggested benefits of the staining system, this might be due to the high porosity of the scaffolds (10) by which diffusion and penetration of the dye through the scaffold structure was facilitated. Stained color intensity was higher for the samples using 2 mmol L^{-1} heparin for conjugation (Fig. 1c) compared to those using 1 mmol L^{-1} heparin (Fig. 1b). However, by increasing heparin concentration to 4 mmol L^{-1} , stained color intensity was inversely decreased (Fig. 1d). The unexpected outcome could be explained in terms of the intrinsic properties of the coupling system and heparin. These include (i) the absence of spacers protruding from scaffold surfaces when applying carbodiimide chemistry for heparin conjugation (19), and (ii) a relatively large and complex structure containing numerous scattered disaccharide units of heparin (20). Consequently, grafting of heparin

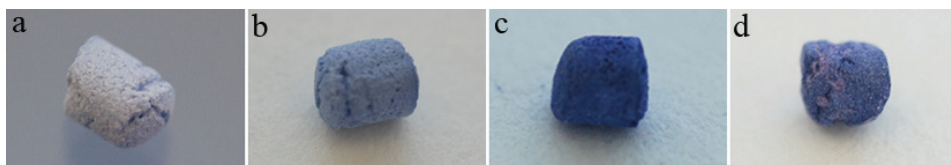


Fig. 1. Representative photographs of the heparin conjugated scaffolds stained with toluidine blue: a) the no-heparin containing scaffold, b) scaffolds processed using 1 mmol L^{-1} , c) 2 mmol L^{-1} and d) 4 mmol L^{-1} heparin solution.

Table I. Evaluation of heparin binding to the scaffolds

Initial conc (mmol L ⁻¹)	Initial amounts (mg in 200 μL) ^a	Conc. after incubation (mmol L ⁻¹)	Unbound amounts (mg in 150 ± 7 μL) ^b	Bound amounts (mg on 4 scaffolds)	Amount bound per scaffold (nmol)	Conjugation efficiency (%)	Clotting appearance ^c
1.0	1	0.84 ± 0.08	0.63 ± 0.029	0.37 ± 0.007	18.5 ± 0.4	37.0 ± 0.7	++
2.0	2	1.75 ± 0.13	1.31 ± 0.061	0.69 ± 0.015	34.0 ± 0.8	34.5 ± 0.8	++
4.0	4	3.70 ± 0.22	2.78 ± 0.130	1.22 ± 0.032	61.0 ± 1.6	30.5 ± 0.8	++

^a Four scaffolds were incubated in 200 μL of heparin solution.

^b The volume of heparin solution drawn out using a measuring microliter syringe after 4 h of incubation.

^c Symbols: ++, + or - indicates truly clotted, slightly clotted or un-clotted status of the PRP, respectively.

onto scaffold surfaces might be ineffective, hindered and further prevented when heparin concentrations are progressively increased, leading to a reduction of surface bound heparin (21) and thereby diminution of dye staining, as shown in Fig. 1d. Using the quantitative method of Smith *et al.* (14), approximately 18–61 nmoles heparin binding to each scaffold were determined. These values corresponded to 30–37 % binding efficiency (Table I). Again, increased binding efficacy was not directly proportional to the heparin concentration initially added in the conjugation reaction. To explain this, the rationales described previously could be applied. Consequently, the concentration of 4.0 mmol L⁻¹ heparin was not further taken into consideration.

Heparin is an anticoagulant. The stability of heparin bonding was then tested to ascertain blood compatibility of the conjugated scaffolds using the PRP assay. Results are shown in Table I, indicating that complete clotting of PRP was visualized in all the test samples. This was due to no heparin present, estimating that leaching away of surfaced heparin into the shaken medium did not occur. Thus, the newly formed covalent bonds were satisfactorily stable, providing blood compatible carriers for growth factors. Moreover, distortion of the scaffold's 3D-structure was not detected after immersion in PBS for 4 weeks or in the process of heparin conjugation (data not shown).

Loading and release of rhBMP-2

To reduce loss of rhBMP-2 activity, the supplied protein was first reconstituted in water containing BSA using the aseptic technique. This stock solution could then be diluted with other aqueous buffers and stored at 4 °C for 1 week or at -20 °C for future applications. In this study, the protein stock solution was diluted to a concentration of 0.4 or 0.8 μmol L⁻¹ in PBS and subsequently employed in the loading experiment. Through simple incubation, interactions between the added rhBMP-2 and conjugated heparin on scaffolds took place. To obtain uniform and reproducible loading, four pieces of conjugated scaffolds in each of the defined groups were immersed in 200 μL of rhBMP-2 solution and incubated for 24 h at 4 °C. Heat induced inactivation of the protein was expected to de-

Table II. Evaluation of rhBMP-2 binding to the scaffolds

Initial conc. ($\mu\text{mol L}^{-1}$)	Initial amounts (μg in 200 μL) ^a	Conc. after incubation ($\mu\text{mol L}^{-1}$)	Unbound amounts (μg in 185 \pm 5 μL) ^b	Bound amounts (μg on 4 scaffolds)	Amount loaded per scaffold (pmol)	Loading efficiency (%)
0.4	2.08	0.18 \pm 0.04	0.86 \pm 0.023	1.22 \pm 0.006	11.73 \pm 0.06	58.7 \pm 0.3
0.8	4.16	0.22 \pm 0.04	1.06 \pm 0.023	3.10 \pm 0.007	29.81 \pm 0.06	74.5 \pm 0.2

^a Four heparin-conjugated scaffolds were incubated in 200 μL of rhBMP-2 solution.

^b The volume of rhBMP-2 solution being drawn out using a microliter syringe after 24 h of incubation.

crease when manipulating it at such a low temperature. Results in Table II show that there were 11.7 and 29.8 pmol of rhBMP-2 bound to each scaffold, corresponding to 58.6 and 74.5 % loading efficiency for the initial loading concentration of 0.4 and 0.8 $\mu\text{mol L}^{-1}$, respectively. It was noted that by increasing the initial protein concentration, increased binding efficacy was observed, but it was not proportional to the initial protein concentration. The amounts of heparin conjugated on a scaffold were most likely in excess compared to that of the bound protein (see Tables I and II). Thus, it might not be crucial for the protein to compete for its binding sites. Although more than 70 % of rhBMP-2 in the 0.8- $\mu\text{mol L}^{-1}$ solution could interact with surfaced heparin, its binding capacity seemed to be limited. Structural information for heparin, BMP-2, and heparin-BMP-2 complexes could be the rationale for explaining the restricted efficiency (22). Heparin is a compound of glycoaminoglycans, which are structurally heterogeneous (23). Native BMP-2 is a homodimeric protein. The BMP-2 subunits are assembled at an angle of approximately 40°; the angle is fairly constant, being stabilized by hydrophobic interactions that take place between these subunits. The N-terminuses of both monomers contain additional five positively charged amino acid residues and function as heparin binding sites (22). The specific affinity of BMP-2 to heparin is then essential for storage, release and protection of the protein from heat, pH and enzymatic degradation (11, 24, 25). Motions of these terminuses are found to be scattered. However, angled monomers are forced to adopt a wider conformation when binding to heparin. Accordingly, changes of rhBMP-2 conformations interacting with heparin on the scaffold might influence the binding affinity for the upcoming protein, ultimately causing such a binding constraint (26).

To imitate the long curing course of most bone fractures, the release of rhBMP-2 from the prepared scaffolds was investigated in PBS for 45 days at 4 °C. In contrast to this study, most researches have explored the release of proteins from delivery systems at 37 °C and often over a shorter time period (27, 28). In fact, during the loading and characterization of the release of rhBMP-2, it is important to ensure that the protein is always in its active form. The temperature of 4 °C was thus specified for the investigations in this project, based on the manufacturer's recommendation. Results indicate that there was no burst release of rhBMP-2 (Fig. 2). 50 % of the protein was released after 2 weeks of incubation in PBS, and more than 90 % of the protein was released after 45 days. Therefore, the *in vitro* results

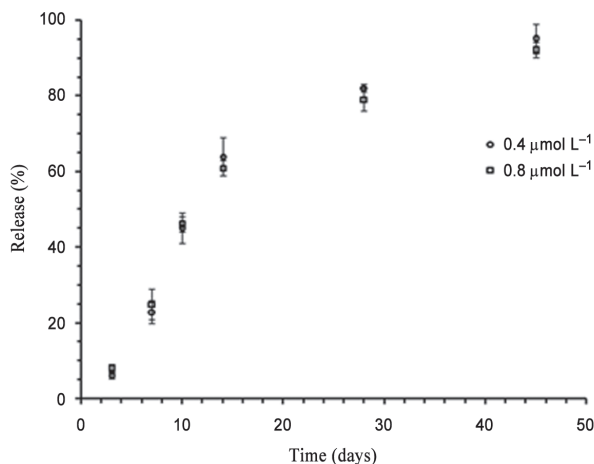


Fig. 2. Release profile of rhBMP-2 from the developed scaffolds in PBS.

suggested a sustained release pattern of the rhBMP-2. For true translation of the *in vitro* data, experiments of biocompatibility and bone regenerative capacity of the established scaffolds will be carried out using a rat model.

Biocompatibility and in vivo osteoinductive capacity of the rhBMP-2 containing scaffolds

The rhBMP-2 loaded scaffolds were investigated for biocompatibility and bone regenerative capacity by being subcutaneously implanted in rats. Histological analysis was carried out after 4 weeks of implantation. Sectioned implants were stained with H&E and alizarin red S, by which the newly formed bone tissue could be distinguished from other soft tissues remaining in the sections. Results are shown in Fig. 3. No presence of macrophage infiltration or tissue inflammation surrounding the implanted sites was found, indicating that the protein delivery system developed in this work was biocompatible and non-toxic. In case of scaffolds lacking both heparin and rhBMP-2, new bone formation was absent (Fig. 3, Gr. 1). Instead, for the scaffolds with an identical amount of heparin conjugates, the amount of newly formed bone was increased in association with increased amount of bound rhBMP-2 (see Gr. 2–4 and Gr. 5–7).

The Interchim[®] assay kit was used for precise determination of the amounts of calcium deposited on histological sections. Results are reported as the degree of mineralization in Fig. 4. Mineralization was not apparent for the samples lacking both heparin and rhBMP-2 (Gr. 1). For the implants containing only heparin conjugates, high mineralization was consistent with the high heparin content (Gr. 2 and Gr. 5). As demonstrated, an approximately 2-fold increase of mineralization was observed for the Gr. 5 implants compared to those of Gr. 2. Moreover, for the heparin-rhBMP-2 bearing implants, more improvement of calcium deposition was clearly observed (Gr. 3–4 and Gr. 6–7). Therefore, ectopic bone formation was successfully induced by a minute amount of rhBMP-2 released into the surrounding tissues of the implant sites (Fig. 2). In contrast, a systemic infusion

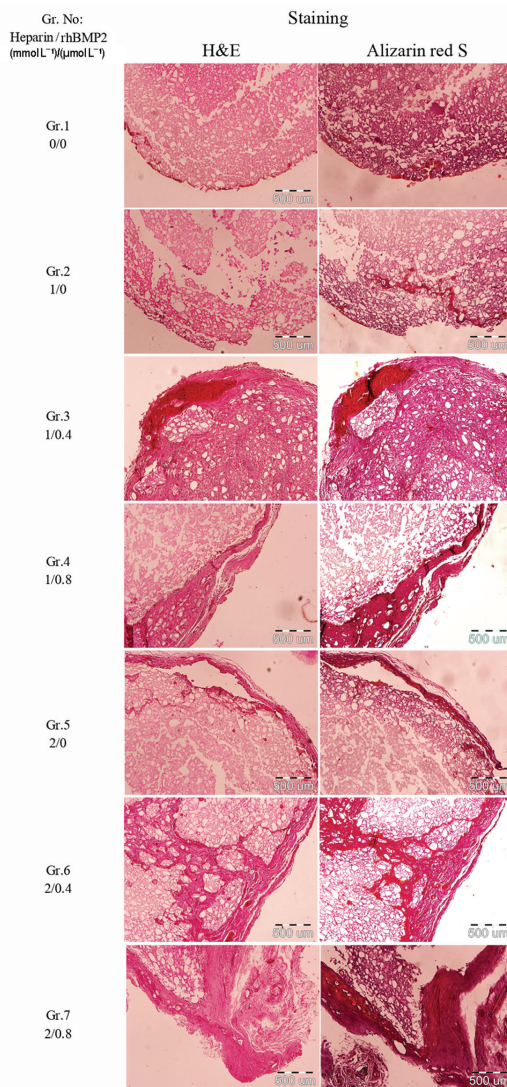


Fig. 3. Representative photographs of sectioned implants after hematoxylin/eosin (H&E) and alizarin red S staining. Test scaffolds were subcutaneously implanted in rats and excised after 4 weeks. Seven groups of scaffold samples were assigned, with regard to the heparin concentration used in the conjugation process (1 or 2 mmol L⁻¹) and that of rhBMP-2 for subsequent loading (0.4 or 0.8 μ mol L⁻¹). The scale bar indicates 500 μ m.

dose of 2 μ g kg⁻¹ day⁻¹ rhBMP-2 in rats did not show any significant inducing effects on serum osteocalcin levels and bone formation (29). However, larger animals are presumed to require greater amounts of BMP-2 for effective osteogenesis than those utilized by small

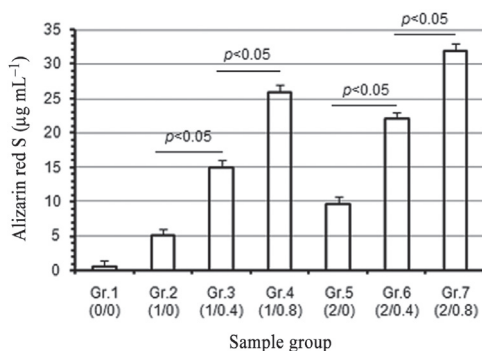


Fig. 4. Quantitative determination of alizarin red S staining in the appertaining sectioned implants.

animals. Comparable bone regenerative capacity of BMP-2 for spinal fusion in dogs has been documented in two different strategies, *viz.*, local application of a dose of 2.3 mg protein at the surgery site and implantation of a collagen scaffold containing 58–920 µg protein (30). Thus, to achieve a satisfactory outcome regarding bone regeneration by BMP-2, protein doses combining local and systemic administration or that to be incorporated in a simple delivery carrier are distinctively higher than those employed in this research.

CONCLUSIONS

As shown in this study, development of scaffolds as delivery systems for critical bone injury is significantly advanced. Scaffolds were constructed by incorporating the Si-CaP powder inside the cross-linked networks of chitosan and TPP. In MES buffer containing EDC and NHS reagents of the carbodiimide reaction, the residual $-NH_2$ ends of chitosan on the scaffolds and the $-COOH$ ends of heparin were activated and concurrently bonded, resulting in scaffolds with surfaced heparin. These newly formed bonds were stable during vigorous washing and extended storage of at least 4 weeks. Binding of rhBMP-2 and the conjugated heparin by ionic interactions occurred after soaking this scaffold in a protein solution. The bioactivity of rhBMP-2 could be preserved, since the protein was not confronted with any harsh conditions. Sustained release of rhBMP-2 was indicated *in vitro*, and its released amounts *in vivo* were sufficient to induce bone regeneration. There were no signs of complications at implanted sites, suggesting that the heparin-rhBMP-2 bearing scaffolds developed in this study were biocompatible, osteoinductive and cost effective.

Acknowledgements. – This work was supported by the National Research University Project of Thailand's Office of the Higher Education Commission, the Nanotechnology Center (NANOTEC), NSTDA, Ministry of Science and Technology, Thailand, through its program of the Center of Excellence Network on Drug Delivery System, and the Graduate School of the Prince of Songkla University.

Animal rights and informed consent

All experiments using animals were in keeping with the local ethics committee guidelines and were conducted with permission.

Conflict of interest

The Si-CaP particles were synthesized by Suphanee Thanyaphoo and used only in our laboratory under the supervision of Associate Professor Dr. Jasadee Kaewsrichan. The authors declare no conflicts of interest for the newly developed scaffolds.

REFERENCES

1. P. P. Spicer, J. D. Kretlow, S. Young, J. A. Jansen, F. K. Kasper and A. G. Mikos, Evaluation of bone regeneration using the rat critical size calvarial defect, *Nat. Protoc.* **7** (2012) 1918–1929; DOI: 10.1038/nprot.2012.113.
2. D. Hadjidakis and I. Androulakis, Bone remodeling, *Ann. N. Y. Acad. Sci.* **1092** (2006) 385–396; DOI: 10.1196/annals.1365.035.
3. J. M. Wozney and V. Rosen, Bone morphogenetic protein and bone morphogenetic protein family in bone formation and repair, *Clin. Orthop.* **346** (1998) 26–37.
4. J. G. Devine, J. R. Dettori, J. C. France, E. Brodt and R. A. McGuire, The use of rhBMP in spine surgery: Is there a cancer risk?, *Evid Based Spine Care J.* **3** (2012) 35–41; DOI: 10.1055/s-0031-1298616.
5. N. E. Epstein, Complications due to the use of BMP/INFUSE in spine surgery: The evidence continues to mount, *Surg. Neurol. Int.* **4** (2013) S343–S352; DOI: 10.4103/2152-7806.114813.
6. J. W. Hustedt and D. J. Blizzard, The controversy surrounding bone morphogenetic proteins in the spine: a review of current research, *Yale J. Biol. Med.* **87** (2014) 549–561.
7. J. O. Hollinger, H. Uludag and S. R. Win, Sustained release emphasizing recombinant human bone morphogenetic protein-2, *Adv. Drug Deliv. Rev.* **31** (1998) 303–318; DOI: 10.1016/S0169-409X(97)00126-9.
8. D. S. Keskin, A. Texcaner, P. Korkusuz, F. Korkusuz and V. Hasirci, Collagen-chondroitin sulfate-based PLLA-SAIB-coated rhBMP-2 delivery system for bone repair, *Biomaterials* **26** (2005) 4023–4034; DOI: 10.1016/j.biomaterials.2004.09.063.
9. M. P. Ginebra, T. Traykova and J. A. Planell, Calcium phosphate cements as bone drug delivery systems: A review, *J. Control. Release* **113** (2006) 102–110; DOI: 10.1016/j.jconrel.2006.04.007.
10. S. Thanyaphoo and J. Kaewsrichan, Synthesis and evaluation of novel glass ceramics as drug delivery systems in osteomyelitis, *J. Pharm. Sci.* **101** (2012) 2870–2882; DOI: 10.1002/jps.23230.
11. I. Capila and R. J. Linhardt, Heparin-protein interactions, *Angew.Chem. Int. Ed. Engl.* **41** (2002) 391–412; DOI: 10.1002/1521-3773(20020201)41:3<390::AID-ANIE390>3.0.CO;2-B.
12. D. R. Bhumkar and V. B. Pokharkar, Studies on effect of pH on cross-linking of chitosan with sodium tripolyphosphate: A technical note, *AAPS PharmSciTech.* **7** (2006) E138–E143; DOI: 10.1208/pt070250.
13. B. Dick, K. G. Schmidt, D. Eisenmann and N. Pfeiffer, A new method for direct detection of heparin on surface-modified intraocular lenses: A modification of Jaques' toluidine blue staining method, *Ophthalmologica* **211** (1997) 75–78.
14. P. K. Smith, A. K. Mallia and G. T. Hermanson, Colorimetric method for the assay of heparin content in immobilized heparin preparations, *Anal. Biochem.* **109** (1980) 466–473.
15. H. Liu and C. Gao, Preparation and properties of ionically cross-linked chitosan nanoparticles, *Polym. Adv. Technol.* **20** (2009) 613–619; DOI: 10.1002/pat.1306.
16. S. Murugesan, J. Xie and R. J. Linhardt, Immobilization of Heparin: Approaches and Applications, *Curr. Top Med. Chem.* **8** (2008) 80–100.
17. E. Laemmel, J. Penhoat, R. Warocquier-Clérout and M. F. Sigot-Luizard, Heparin immobilized on proteins usable for arterial prosthesis coating: growth inhibition of smooth-muscle cells, *J. Biomed. Mater. Res.* **39** (1998) 446–452; DOI: 10.1002/(SICI)1097-4636(19980305)39:3<446::AID-JBM14>3.0.CO;2-8.

18. P. B. van Wachem, J. A. Plantinga, M. J. Wissink, R. Beernink, A. A. Poot, G. H. Engbers, T. Beugeling, W. G. van Aken, J. Feijen and M. J. van Luyn, In vivo biocompatibility of carbodiimide-crosslinked collagen matrices: Effects of crosslink density, heparin immobilization, and bFGF loading, *J. Biomed. Mater. Res.* **55** (2001) 368–378; DOI: 10.1002/1097-4636(20010605)55:3<368::AID-JBM1025>3.0.CO;2-5.
19. Z. Grabarek and J. Gergely, Zero-length crosslinking procedure with the use of active esters, *Anal. Biochem.* **185** (1990) 131–135; DOI: 10.1016/0003-2697(90)90267-D.
20. R. J. Linhardt, Perspective: 2003 Claude S. Hudson Award Address in Carbohydrate Chemistry. Heparin: Structure and Activity, *J. Med. Chem.* **46** (2003) 2551–2554; DOI: 10.1021/jm030176m.
21. T. Y. Liu, L. Y. Huang, S. H. Hu, M. C. Yang and S. Y. Chen, Core-Shell Magnetic Nanoparticles of heparin conjugate as recycling anticoagulants, *J. Biomed. Nanotechnol.* **3** (2007) 353–359; DOI: <http://dx.doi.org/10.1166/jbn.2007.044>.
22. R. Ruppert, E. Hoffmann and W. Sebald, Human bone morphogenetic protein 2 contains a heparin binding site which modifies its biological activity, *Eur. J. Biochem.* **237** (1996) 295–302; DOI: 10.1111/j.1432-1033.1996.0295n.x.
23. U. Lindahl and L. Kjellen, Heparin or heparan sulfate – what is the difference?, *Thromb. Haemost.* **66** (1991) 44–48.
24. R. Guan, X. L. Sun, S. Hou, P. Wu and E.L. Chaikof, A glycopolymer chaperone for fibroblast growth factor-2, *Bioconjug. Chem.* **15** (2004) 145–151; DOI: 10.1021/bc034138t.
25. T. Takada, T. Katagiri, M. Ifuku, N. Morimura, M. Kobayashi, K. Hasegawa, A. Ogamo and R. Kamijo, Sulfated polysaccharides enhance the biological activities of bone morphogenetic proteins, *J. Biol. Chem.* **278** (2003) 43229–43235; DOI: 10.1074/jbc.M300937200.
26. C. Scheufler, W. Sebald and M. Hülsmeier, Crystal structure of human bone morphogenetic protein-2 at 2.7 Å resolution, *J. Mol. Biol.* **287** (1999) 103–115; DOI: 10.1006/jmbi.1999.2590.
27. X. Li, J. Xu, T. M. Filion, D. C. Ayers and J. Song, pHEMA-nHA encapsulation and delivery of vancomycin and rhBMP-2 enhances its role as a bone graft substitute, *Clin. Orthop. Relat. Res.* **471** (2013) 2540–2547; DOI: 10.1007/s11999-012-2644-5.
28. E. R. Balmayor, G. A. Feichtinger, H. S. Azevedo, M. van Griensven and R. L. Reis, Starch-poly-ε-caprolactone microparticles reduce the needed amount of BMP-2, *Clin. Orthop. Relat. Res.* **467** (2009) 3138–3148; DOI: 10.1089/ten.2006.0194.
29. E. Zerath, X. Holy, B. Noël, A. Malouvier, M. Hott and P. J. Marie, Effects of BMP-2 on osteoblastic cells and on skeletal growth and bone formation in unloaded rats, *Growth Horm. IGF Res.* **8** (1998) 141–149.
30. H. S. Sandhu, L. E. Kanim, J. M. Kabo, J. M. Toth, E. N. Zeegen, D. Liu, R. B. Delamarter and E. G. Dawson, Effective doses of recombinant human bone morphogenetic protein-2 in experimental spinal fusion, *Spine (Phila Pa 1976)* **21** (1996) 2115–2122.